crystals

MDPI

Article

Ancient Metallurgical Iron Slags—Chemical, Powder X-ray Diffraction and Mössbauer Spectroscopic Study

Bilyana Kostova [1,*], Daniela Paneva [2], Zara Cherkezova-Zheleva [2], Katerina Mihaylova [1,3] and Boyan Dumanov [4]

1 Department of Natural Sciences, New Bulgarian University, 21 Montevideo Blvd., 1618 Sofia, Bulgaria; kate_mih@imc.bas.bg
2 Institute of Catalysis, Bulgarian Academy of Sciences, Acad. G. Bonchev Str., bldg.11, 1113 Sofia, Bulgaria; daniela@ic.bas.bg (D.P.); zzhel@ic.bas.bg (Z.C.-Z.)
3 Institute of Mineralogy and Crystallography, Bulgarian Academy of Sciences, Acad. G. Bonchev Str., bldg.107, 1113 Sofia, Bulgaria
4 Department of Archaeology, New Bulgarian University, 21 Montevideo Blvd., 1618 Sofia, Bulgaria; bdumanov@nbu.bg
* Correspondence: bkostova@nbu.bg

Abstract: The production and trade of metals was the foundation of the economic wealth of many regions in the world, which makes the study of ancient metallurgical slags of primary importance. This type of study is relatively new for Bulgaria, where research in the field started in the late 1960s with chemical analysis of copper ore, slags, tools and finished goods from the ancient copper mine in the Ay-bunar area. Iron is one of the most commonly found elements in the earth's crust and its deposits are widespread, including on Bulgaria's territory. To this day, however, the study of iron slags from Bulgarian sites through chemical and phase analysis has almost never been explored. The application of these methods allows for the determination of the technology of the ancient metallurgical process. This study investigates iron slags from two Bulgarian archaeological sites, situated in close proximity to the Sarnevets hematite ore deposit, Sarnena Sredna Gora mountain. The ore bodies of the deposit outcrop on the earth's surface and can be easily recognized due to the red coloring of the soil around them, which is a characteristic trait for finding iron deposits. In addition to the ancient mining activities in the region, proven by over 20 registered ancient mine workings, ancient metallurgical activities were established as well, as proven by the discovered slags. A sample from the hematite ore was studied along with the slags, so that the percentage of iron extracted during the metallurgical process can be determined. The samples were studied through X-ray fluorescence analysis, powder X-ray diffraction analysis, and Mössbauer spectroscopy. The obtained results show that the slags are of the "furnace bottom slags" type, which is a product of metallurgical activity achieved through bloomery technology. The temperature range of the furnaces was determined to be around 900–1100 °C. The reduction of iron was possible at such low temperatures due to the ore's type—self-fluxing hematite ore. The percentage of iron extracted from the ore was calculated to be between 3.39% and 8.65%. Additionally, a relationship was established between the percentage of extracted iron, the Fe^{2+} content included in wüstite, and the viscosity index of the liquid slag. The acquired results are new to the archaeological studies conducted on Bulgaria's territory and are a prerequisite for future interpretation and archaeological research.

Keywords: Bulgarian ancient iron metallurgical slags; Mössbauer spectroscopy; powder X-ray diffraction

check for updates

Citation: Kostova, B.; Paneva, D.; Cherkezova-Zheleva, Z.; Mihaylova, K.; Dumanov, B. Ancient Metallurgical Iron Slags—Chemical, Powder X-ray Diffraction and Mössbauer Spectroscopic Study. *Crystals* **2023**, *13*, 888. https://doi.org/10.3390/cryst13060888

Academic Editors: Hongbin Bei and Raphaël P. Hermann

Received: 23 April 2023
Revised: 25 May 2023
Accepted: 26 May 2023
Published: 28 May 2023

1. Introduction

Iron is one of the most common elements in the earth's crust, which determines the geographically widespread mining of iron in the past [1]. There are two known metallurgical processes for iron mining, which use two types of furnaces. The first one uses a bloomery furnace (perhaps 1 or 2 m high) and was implemented from the 8th century

BC until the 16th century AD, and later in some areas. After the 15th century AD, blast furnaces appeared [1]. Meteoritic iron might have been forged in copper alloy designed furnaces, but these would have remained isolated and expensive occurrences [2].

Bloomery technology, the most ancient method for iron extraction, is a direct method. During this process, iron would be extracted in solid state through reduction at a maximum temperature of 1200 °C [3]. The reduction would include part of the iron oxides from the ore until the formation of a mechanical solid mixture (bloom) from a solid metal sponge iron mixed with slag. About 10–20% of the iron in the ore was usually recovered by this method [4], which also led to the creation of iron-rich slags. The use of bloomery technology allowed for iron to be extracted without having to melt it (~1550 °C), which requires a temperature that was impossible to reach at the time, due to the lack of a high-calorie fuel and the imperfect constructions of the furnaces. Flux (limestones, quartz sands, sandstones) was often added to the ore during the metallurgical process in order to reduce the reduction temperature of the iron and increase its extraction rate. By using fluxes, iron reduction would start at around 800 °C [5]. Wood charcoal was used as fuel for the furnaces, which also served as a reducing agent in the system [3,5–7]. Control of redox conditions in the furnace was achieved by moderate air supply [8] and a high charcoal/ore ratio in the furnace [9].

The first iron reduction furnaces (bowl furnaces; bowl-shaped hearths) date back to the Early Iron Age. They comprised a pit in the soil or in the rocks, in which a mixture of ore and charcoal was placed, and the whole structure was covered with clay. There was a tuyere for direct oxygen supply from the bellows, but no slag tap-hole. Furthermore, wind-powered furnaces have also been used, situated at appropriate places in upland and mountainous regions. With this design, the temperature in the furnace reached a maximum of 1150 °C. After the completion of the metallurgical process, the clay structure was completely demolished, the bloom taken out, and the pit was cleaned of the slag. Shaft furnaces were used during this time as well, again without a slag tap-hole. The advantage of these furnaces was that they offered a more sustainable preservation of the reducing conditions in the furnace. During the Roman Age, the design of the bowl furnace changed—its diameter and height increased, and more than one tuyere and slag tap-hole were added. It is assumed that slag tapping was universal in the territories colonized by the Romans, and it is considered that in certain places these furnaces were used without any modifications in their structures until the medieval period [9]. In the iron reduction process, the slag was the only liquid component in the system. The sponge iron has a higher density than the liquid slag, which transported the small metal particles to the walls of the furnace, where they coalesced and formed larger volumes of bloom or lumps [5,9]. With regard to this, slags may contain different phases: (i) phases obtained by thermal reaction with inclusions from the ore (depending on the type of ore), with molten materials from the furnace (clay coating), with inclusions from the fuel and ash from its burning, and with the material used for flux and (ii) phases obtained in solid state depending on the oxidation-reduction conditions in the furnace (the type of these phases is controlled by the amount of air supplied to the furnace). This method of iron production defines the main ferrosilicate content of the slags, which is similar to that of fayalite (Fe_2SiO_4) and is formed during a reaction of FeO and Si from quartz [5,10].

The use of the blast furnace (Catalan forge) began from the 15th century AD. Higher temperatures were reached through these furnaces, into which flux was added (sand or limestone) and molten iron was obtained. Wood charcoal was used as fuel until the 18th century, at which point coke started being used as well. The blast furnaces were much bigger in size than the bloomery ones—they were masonry towers with an area of 5-6 m^2 and a height of around 6 m, which provided a more reducing atmosphere and consequently led to a higher degree of iron extraction. As a result of this more advanced construction, the produced metallurgical slags were high in silicon and low in iron [1].

Archaeological iron slags include furnace and smithing slags. There are several types of furnace slags: bottom slags (slags remaining at the bottom of the furnace until the end of

the metallurgical process), bloomery slags (slags that are part of the bloom), tapped slags (slags taken out of the furnace in liquid state during the metallurgical process—they cool significantly faster than bottom slags). All furnace slags are metallurgical, formed in the furnace during the reduction of iron. Furnace bottom slags are spread at the bottom of the furnace, in direct contact with the fuel, the furnace's ceramic coating, and the fuel's ash, which allows for the inclusion of components from these in the slag's composition. These slags are voluminous, with a spongy structure [11]. Bloom, made from sponge iron and bloomery slags, is placed on the furnace bottom slags. These slags are separated from the sponge iron through hammering [9]; they have a spongy structure and a plano-convex shape with 2–5 cm thickness from the hammer's blows [12]. During the construction of the furnace, which includes slag tap-holes, smelting (tapped) slags are formed. The tapped slags are thin with a mirror-smooth surface with evidence of flowing [2]. The smithing slags are formed during the process of forging the sponge iron [9]. The furnace and smithing slags are the product of two different pyrometallurgical processes: the metallurgical process requires a reducing environment, and the smithing process requires an oxidizing environment [9], which determines their different phase composition [5].

By studying the ancient slags, the technology of the metallurgical process for iron extraction can be determined—the furnace type, the redox conditions and the temperature. The outer microscopic marks of the slags can help in many cases, but the conclusions that can be made from them are too few. For a detailed study of the slags, the use of chemical and phase analysis is required, for example by using powder X-ray diffraction analysis and Mössbauer spectroscopy [6,10].

The study of traces from ancient metallurgical processes is a relatively new research field for Bulgaria. It started towards the end of the 1960s with the study of copper ore, slags, tools, and finished goods from the ancient copper mine in the Ay-bunar region. The research included chemical analysis of the aforementioned objects as well. These studies prove the use of rare metals such as meteoric iron before the beginning of the Early Iron Age [13]. Archaeological research on iron mining in Bulgaria, including data from the chemical analysis of iron slags, was recently published by Dumanov [14]. Nevertheless, at present, publications on iron slags from Bulgaria including data on their chemical and phase composition are sporadic. Slag research is an important issue since the production and trade of metals was the foundation of the economic wealth of many regions in the world.

This work deals with four samples of iron slags from two Bulgarian archaeological sites (Malko Dryanovo and Sladak Kladenets) in order to determine the slag types and the conditions in which the metallurgical process was performed (redox conditions, temperature, etc.) Since the sites are situated in close proximity to the Sarnevets iron deposit, a sample from the ore was analyzed as well so as to determine the effectiveness of the ancient metallurgical process (i.e., determining the percentage of iron extracted from the ore). The studies were conducted through X-ray fluorescence (XRF) analysis in order to determine the chemical composition of the slags, powder X-ray diffraction (PXRD) analysis to determine the phase composition, and Mössbauer spectroscopy to determine the phase composition and the percentage content of Fe^{2+} and Fe^{3+} in the individual phases. The obtained results offer new data on ancient iron ore mining in the territory of Bulgaria and an opportunity for archaeological interpretation.

2. Materials and Methods

In Sarnena Sredna Gora (Bulgaria), between the villages of Sarnevets and Malko Dryanovo, an iron hydrothermal deposit called Sarnevets can be found. The ore mineralization contains hematite and a small amount of hydrogoethite, with the ore bodies outcropping on the ground's surface [15]. The direct outcrop of the ore bodies on the earth's surface is marked by a characteristic red coloring of the soils (Figure 1). More than 20 surface ancient mine workings of different sizes and depths have been registered in the area of the deposit [16] (Figure 1), and iron slags have been found in the nearby archaeolog-

ical sites. These data shows the development of ancient mining and metallurgical activity in the area.

Figure 1. Red soils as a result of iron mineralization and traces of ancient ore mining (Gure Tepe peak, Dupkata region, located between Sarnevets and Malko Dryanovo villages).

The archaeological sites of Sladak Kladenets and Sarnevets are positioned in close proximity to the ore deposit. In both sites, iron slags were found on the surface. Two slag samples from each of the sites were examined—No. 116-1 and No. 116-2 from Sladak Kladenets and No. 131-1 and No. 131-2—from Malko Dryanovo. All found slags are voluminous, porous, with a high relative weight and oxidation and limonitization (a chemical weathering process that occurs under atmospheric conditions, where a ferrous iron phase transforms into a ferric iron phase) on the surface (Figure 2). No traces of metallurgical furnaces were found in the sites. Chronologically, it is assumed that the metallurgical activity was conducted probably during the Late Roman Age, Late Antiquity, and the Middle Ages, while not excluding the possibility of iron mining in the 1st millennium BC [17]. One sample of the Sarnevets deposit's ore was examined—sample No. 112.

Figure 2. Ancient slags.

X-ray fluorescence (XRF) analysis was performed using a spectrometer WD-XRF Supermini 200 - Rigaku, Japan (50 kV and 4mA, 200 W X-ray tube with Pd-anode, 30 mm^2) in a helium atmosphere. Two different X-ray detectors, a gas flow proportional counter for light elements and a scintillation counter for heavy elements, were used. Depending on the wavelength range, two analyzing crystals: LIF 200 (for Ti-U), PET (for Al-Ti) and RX25 (for F-Mg) were used. The software package ZSX was used for data processing. The samples were prepared as tablets with CEREOX-BM-0002-1 powder.

Powder X-ray diffraction (PXRD) analysis was performed using Empyrean, "Panalytical", CuKα radiation (λ = 0.15418 nm) (operating at 40 kV, 30 mA) from 5 to 90° 2θ with a step of 0.013 2θ, 30 s/step with the pulse height distribution (PHD) refinement, starting from 25, 30, 35, 40, 41 to 51 % and the optimal value selection. Phase identification and peak fitting were carried out using the computer program for qualitative analysis QualX (v. 2.24) with the indexed Powder Diffraction File database [18].

^{57}Fe Mössbauer measurements were performed using a spectrometer (Wissenschaftliche Elektronik GmbH, Starnberg, Germany), operating in a constant acceleration mode. Transmission Mössbauer spectra were measured with an analyzer with 1024 channels. The used ^{57}Co/Rh isotope's activity was 15 mCi. α-Fe foil absorber with thickness of 30 µm and linewidth 0.27 mm/s was used for calibration. The samples were adjusted to an optimum thickness for a "thin" absorber density of about 10 mg/cm^{-2} of the total iron content. The

Mössbauer spectra were recorded at room temperature (293 K) over a velocity range of ±10 mm/s for 24-48 hours. The hyperfine interactions parameters were determined via computer fitting with Lorentzian lineshapes using the program NORMOS (based on the least squares method): isomer shift (δ) relative to α-Fe, quadrupole shift (2ε) /quadrupole splitting (Δ), hyperfine magnetic field (Bhf). In addition, widths (Γ) and component relative areas (A) were also calculated. The calculated errors for δ, 2ε, Δ, and Γ are ±0.01 mm/s, and for B_{hf} is ± 0.1T.

3. Results

3.1. XRF

The results from the XRF analysis are presented in Table 1. In the slag samples, Fe_2O_3 (from 43.93 to 51.46%) and SiO_2 (from 26.80 to 32.58%) have the highest percentage content. The iron contents in the slags are lower than those in the ore. The amount of Al_2O_3 in the slags is slightly higher than that in the hematite ore, except for sample No. 116-2, in which there is an increased amount of calcium. Magnesium, manganese, and titanium are present in approximately equal concentrations in the hematite ore and in the slags. Sodium, potassium, calcium, phosphorus, and sulfur in the slags are in significantly higher amounts than in sample No. 112.

Table 1. XRF results (mass %).

Sample	Na_2O	MgO	Al_2O_3	SiO_2	P_2O_5	SO_3	K_2O	CaO	TiO_2	MnO	Fe_2O_3	Fe *
No 112	<LOD	0.73	6.03	34.50	0.37	<LOD	0.95	0.70	0.27	0.09	56.31	39.37
No. 116-1	0.52	0.48	9.54	32.55	0.68	0.09	4.40	6.28	0.34	0.11	44.90	31.39
No. 116-2	0.70	0.88	5.94	26.80	1.42	0.11	6.07	9.75	0.16	0.16	47.75	33.39
No. 131-1	0.42	0.40	7.12	28.75	0.60	0.13	5.02	5.61	0.24	0.10	51.46	35.98
No. 131-2	0.75	0.78	8.94	32.58	0.70	0.08	5.32	6.39	0.25	0.11	43.93	30.72

LOD—limits of detection. * calculated equivalent mass % Fe

3.2. PXRD

The results from the PXRD analysis are presented in Figure 3 and Table 2. Sample No. 112 has a mineral composition of hematite (#33-0664) and quartz (# 08-7653), which defines the ore as polymineral. All slag samples contain quartz, olivine (fayalite, #76-5937; kirschsteinite, #34-0098), and wüstite (#46-1312). Maghemite is found only in the samples from Sladak Kladenets, magnetite (#19-0629) in the samples from Malko Dryanovo, leucite (#38-1423) in samples No. 116-1, 131-1, and 131-2. Of the weathering minerals (limonites) goethite (#29-0713) and/or lepidocrocite (#76-2301) were proven in all samples, while pyrolusite [19] was only found in sample No. 116-2.

Table 2. XRD results: detected minerals and phases.

Minerals/Phases				Sample				
				Ore	Slags			
Origin	Name		Chemical formula	No. 112	No. 116-1	No. 116-2	No. 131-1	No. 131-2
Ore-forming raw/relict	H—hematite		$Fe^{3+}{}_2O_3$	H	-	-	-	-
	Q—quartz		SiO_2	Q	Q	Q	Q	Q
New-formed metallurgical phases	olivine group	F—fayalite	$Fe^{2+}{}_2SiO_4$	-	F	-	F	F
		K— kirschsteinite	$CaFe^{2+}SiO_4$	-	-	K	-	-
	feldspatoid group	L—leucite	$K(AlSi_2O_6)$	-	L	-	L	L
	Fe-oxides	W—wüstite	$Fe^{2+}O$	-	W	W	W	W
	P—pyrolusite		$Mn^{4+}O_2$	-	-	P	-	-
New-formed during liquid slag cooling	Fe— oxides	Ma— maghemite	γ-$Fe^{3+}{}_2O_3$	-	Ma	Ma	-	-
	M—magnetite		$Fe^{2+}Fe^{3+}{}_2O_4$				M	M
New-formed weathering minerals	G—goethite		α-$Fe^{3+}O(OH)$	-	G	G	G	-
	Le—lepidocrocite		γ-$Fe^{3+}O(OH)$	-	-	Le	-	Le

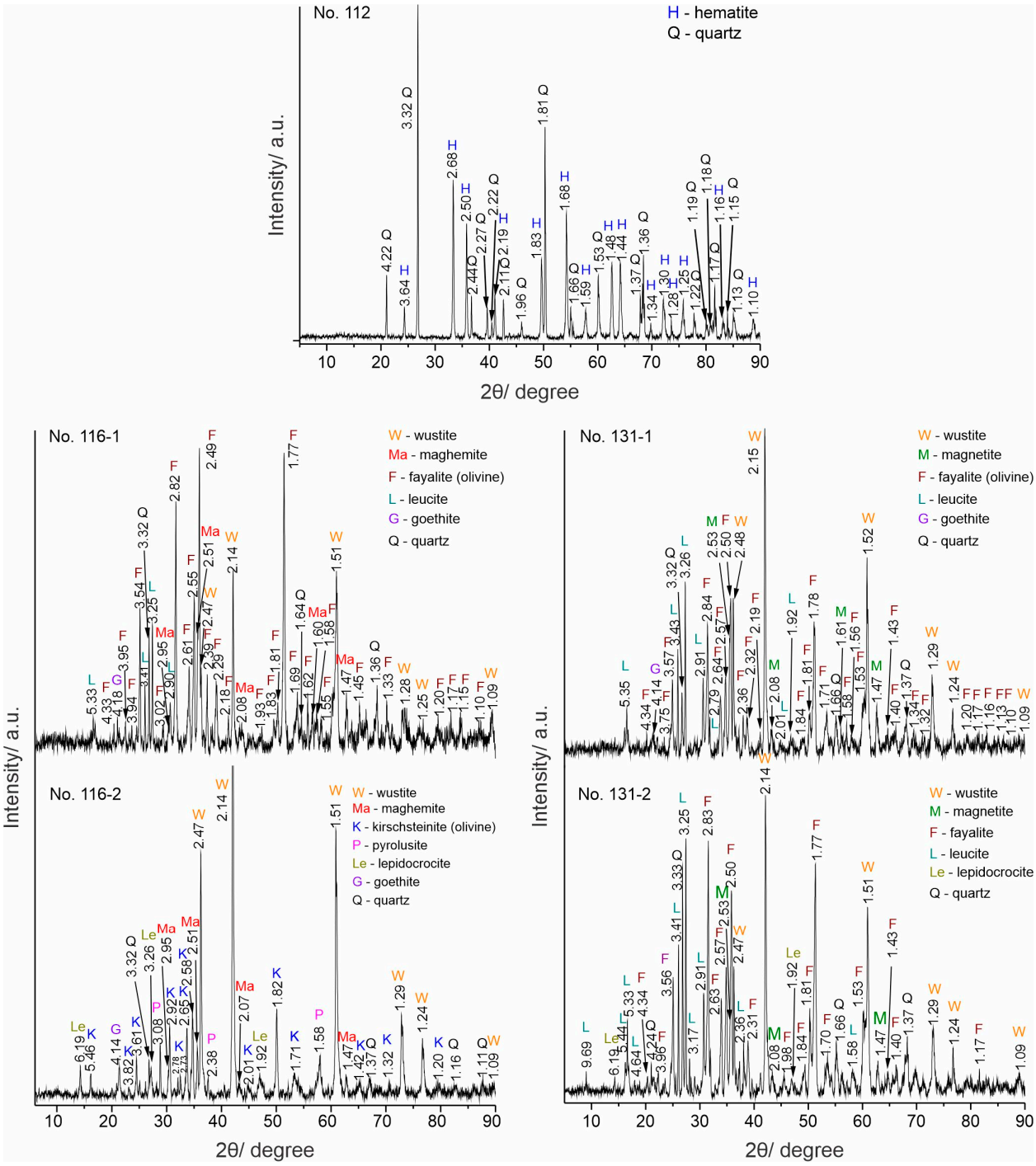

Figure 3. PXRD patterns.

3.3. Mössbauer Spectroscopy

The registered Mössbauer spectra of the studied materials are presented in Figure 4. The fitted parameters are given on Table 3. Numbers of the components forming each Mössbauer spectrum are based on the obtained results from the PXRD phase analysis. The sextet components (Sx) are included in a fitting model for iron-bearing phases with hyperfine magnetic interactions. Doublet components (Db) appear when such interactions are not registered, and the phases have paramagnetic or superparamagnetic properties.

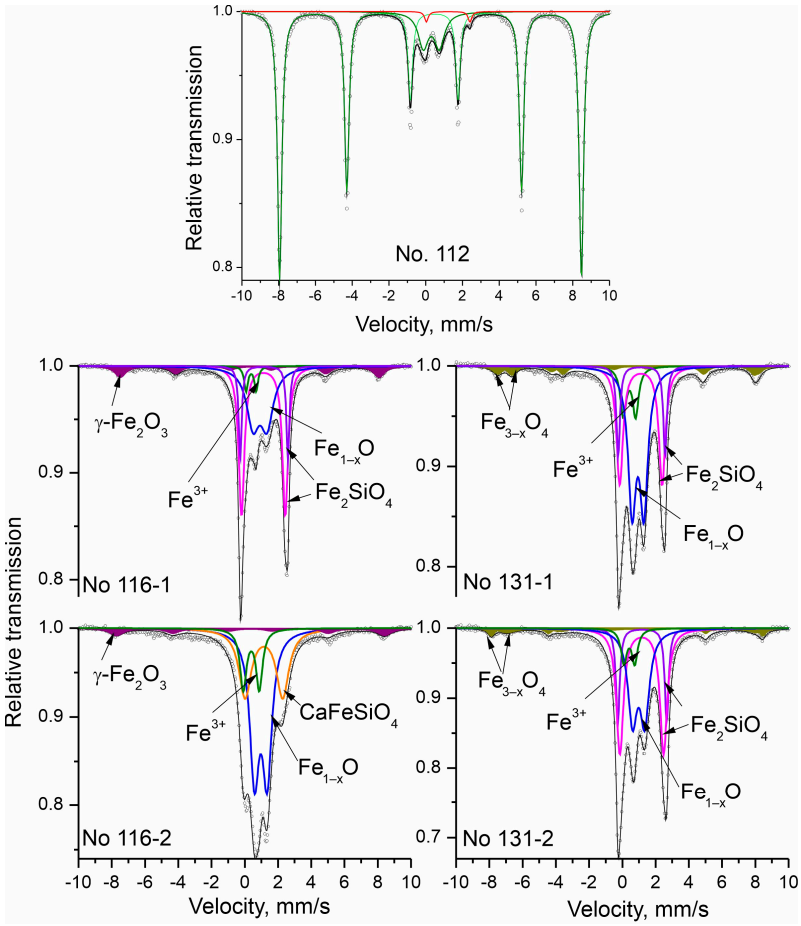

Figure 4. Mössbauer spectra after a fitting procedure.

Table 3. Mössbauer parameters of the investigated samples. The isomer shift values are relative to α-Fe. The computer fitting of the spectra is based on the standard constraints: fit of the magnetic sextets by $A_{1.6}$: $A_{2.5}$:$A_{3.4}$ = 3:2:1, as well as equal values of $\Gamma_{1.6}$, $\Gamma_{2.5}$ and $\Gamma_{3.4}$. The calculated errors for **δ**, 2ε, **Δ**, and Γ are ±0.01 mm/s. The calculated error for B_{hf} is ± 0.1T.

Sample	Compounds	δ, mm/s	2ε/Δ, mm/s	B_{hf}, T	Γ, mm/s	A, %	Fe^{2+}/Fe^{3+}
No. 112	Sx- α-Fe_2O_3 - (Fe^{3+})	0.36	-0.20	50.7	0.31	86	2/98
	Db1 - Fe^{2+}	1.22	2.37	-	0.24	2	
	Db2 - (Fe^{3+})	0.31	0.88	-	0.66	12	
No. 116-1	Sx-γ-Fe_2O_3 - (Fe^{3+})	0.33	0.01	48.3	0.78	11	85/15
	Db1-Fe_2SiO_4 - (Fe^{2+})-M1	1.12	2.63	-	0.41	39	
	Db2-Fe_2SiO_4 - (Fe^{2+})-M2	1.16	2.87	-	0.25	13	
	Db3-$Fe_{1-x}O$ - (Fe^{2+})	0.92	0.84	-	0.92	33	
	Db4- (Fe^{3+})	0.38	0.61	-	0.43	4	
No. 116-2	Sx -γ-Fe_2O_3 - (Fe^{3+})	0.34	0.01	49.9	0.98	7	80/20
	Db1-$CaFeSiO_4$ - (Fe^{2+})-M1	1.15	2.26	-	0.90	32	
	Db2-$Fe_{1-x}O$ - (Fe^{2+})	0.97	0.77	-	0.68	48	
	Db3- (Fe^{3+})	0.39	0.97	-	0.47	13	
No. 131-1	Sx1 - $Fe_{3-x}O_4$- ($Fe^{3+}{}_{tetra}$)	0.29	0.03	48.4	0.69	5	82/18
	Sx2 - $Fe_{3-x}O_4$- ($Fe^{2.5+}{}_{octa}$)	0.65	0.01	45.4	0.62	6	
	Db1-Fe_2SiO_4- (Fe^{2+})-M1	1.12	2.55	-	0.47	27	
	Db2-Fe_2SiO_4- (Fe^{2+})-M2	1.16	2.82	-	0.27	11	
	Db3-$Fe_{1-x}O$- (Fe^{2+})	0.94	0.71	-	0.58	40	
	Db4- (Fe^{3+})	0.42	0.74	-	0.43	10	
No. 131-2	Sx1 - $Fe_{3-x}O_4$- ($Fe^{3+}{}_{tetra}$)	0.29	0.00	49.1	0.46	4	85/15
	Sx2 - $Fe_{3-x}O_4$- ($Fe^{2.5+}{}_{octa}$)	0.59	0.01	45.4	1.20	6	
	Db1-Fe_2SiO_4- (Fe^{2+})-M1	1.16	2.63	-	0.52	36	
	Db2-Fe_2SiO_4- (Fe^{2+})-M2	1.19	2.93	-	0.29	14	
	Db3-$Fe_{1-x}O$- (Fe^{2+})	0.98	0.73	-	0.67	32	
	Db4- (Fe^{3+})	0.40	0.65	-	0.42	8	

Sextet components in the Mössbauer spectra have the parameters of iron oxides, respectively hematite, magnetite, and maghemite [20].

The results of sample No. 112 hematite ore show that it contains mainly Fe^{3+} ions—98%—while the other 2% are Fe^{2+}. The calculated Mössbauer parameter values of the sextet component prove the presence of hematite [20]. The doublet component (Db2) with an isomer shift value of 0.31 mm/s is characteristic of Fe^{3+} ions in paramagnetic and/or superparamagnetic phases due to their critically small particle size. According to the obtained PXRD data, this could be a superparamagnetic hematite phase or/and a paramagnetic substituted hematite. The sextets of the spectra of samples No. 116-1 and No. 116-2 belong to maghemite, while in samples No. 131-1 and No. 131-2 are registered two sextets characteristic of magnetite. At room temperature, the typical Mössbauer spectrum of the γ-Fe_2O_3 (maghemite) compound exhibits two overlapping magnetic sextets related to the tetrahedral (A) and octahedral [B] sites for iron ions. However, the low content of the maghemite phase in the samples, as well as the high content of impurities in the maghemite compound, induces a broadening of the respective resonant curve. Thus, the presence of the closely spaced lines' superposition cannot be exactly associated with the characteristic pattern of tetrahedral (A) and octahedral [B] iron cations. On the other hand, the iron ions in the magnetite structure occupied the octahedral [B] and tetrahedral (A) sites as $(Fe^{3+})[Fe^{3+}Fe^{2+}]O_4$. Magnetite is a member of the so-called mixed valence compounds, where a fast electron hopping between the cations (Fe^{2+} and Fe^{3+}) in the octahedral sublattice is presented at room temperature. Correspondingly, the registered oxidation state of the octahedral coordinated iron ions in their Mossbauer spectra has an average value, i.e., $Fe^{2.5+}$. The ratio of the two spectral areas of the octahedral [B] and tetrahedral (A) components is equal to two for a stoichiometric compound. Thus, the obtained component ratio (Table 3) defines the presence of a nonstoichiometric compound, which can be presented as $Fe_{3-x}O_4$. The determined quantities of the magnetic phases (magnetite for No. 131-1 and No. 131-2 and maghemite for No. 116-1 and No. 116-2) do not differ significantly in these samples. Two types of parameters are determined for their doublet components, which are typical for iron ions in the second and third oxidation states. The doublets related to the presence of Fe^{2+} refer to two types—wüstite and olivine (fayalite and kirschsteinite). The wüstite amount is different in the four samples—in the range of 32–48%. Apart from the wüstite content, there are also differences in its non-stoichiometry and crystallinity. The line width in the Mössbauer spectra is directly related to the crystallinity of the respective phase. The comparison of the lines for the same phase in the four samples indicates that wüstite crystallinity is the lowest in sample No. 116-1, and the highest in sample No. 131-1. Considering that wüstite's quadrupole splitting is proportional to the presence of nonferrous ions and vacancies, then the wüstite in sample No. 116-1 has the highest degree of non-stoichiometry. The degree of non-stoichiometry is relatively similar for the rest of the samples and is lower than that of sample No. 116-1. Lines belonging to an iron silicate—fayalite/olivine—are registered in three of the samples (Table 3). In them, the iron ions occupy two non-equivalent positions, M1 and M2, which have different symmetry. This is the reason that, in fayalite's Mössbauer spectra, two doublets are registered with different values of the quadrupole splitting and approximately equal areas. As a result, two doublets for fayalite are included in Table 3 [21]. From the data presented, it can be seen that in all three samples containing fayalite, there are deviations from the uniform occupation of the positions M1 and M2 by the iron ions—M1 is much more populated than M2. Through PXRD, the presence of kirschsteinite is proven in sample No. 116-2. It is characterized by a Mössbauer spectra with one doublet, which has lower values of quadrupole splitting than those of fayalite [22].

The doublet components in all samples, whose isomer shift values are within the range 0.31–0.42 mm/s, are characteristic of Fe^{3+} ions. They can be found in different phases, but due to the similar values of the Mössbauer spectra an overlapping occurs. All iron oxides and hydroxides that have critically small particle sizes and are superparamagnetic can be referred with this component. The second group of compounds contributing to this

component are iron-bearing minerals identified by PXRD that contain Fe^{3+} due to their partial oxidation. In PXRD, goethite and lepidocrocite were registered in all four samples. In the Mössbauer spectra, the component Db - (Fe^{3+}) has the highest content in sample No. 116-2—13%. Both iron hydroxides—goethite and lepidocrocite—were identified for the same sample. Therefore, it can be assumed that iron hydroxides, including superparamagnetic ones, have a greater contribution to this component.

4. Discussion

4.1. Slag Type

All examined slags are voluminous, with pores throughout the volume and on the surface, and a visible oxidation crust (Figure 2). According to these characteristics, they can be defined as metallurgical furnace bottom slags or smithing slags [3]. Wüstite is a phase formed under reducing conditions, in which the metallurgical process takes place. If the thermal process performed done in a completely oxidizing environment (the smithing process), then magnetite would have formed instead of wüstite [7]. Apart from wüstite, fayalite was found in the slags as well, with both of these phases being present in high amounts (Table 3), which proves the relatively slow cooling of the slags [11]. These results define the studied slags as metallurgical, "furnace bottom slags". The analyzed slags have a ferrosilicate content similar to that of fayalite and have a high amount of Fe_2O_3 (Table 1), which proves that they were obtained through a metallurgical process in a bloomery furnace [1,5,10].

4.2. Slag Phase Composition

The phase composition of the slags includes: (i) newly formed metallurgical phases (olivine, leucite, wüstite, pyrolusite); (ii) newly formed phases during the cooling of the slag (maghemite, magnetite) [12]; (iii) newly formed weathering phases (goethite, lepidocrocite); and (iv) a relict phase from the raw ore—quartz (Table 2).

Olivine was proven in all samples, and leucite in three of them. The elements Ca, Al, and K were involved in their formation. The higher Ca and Al content in the slags, in comparison with the sample from the ore (No. 112), suggests a combined origin of these elements—from wood charcoal and from the ceramic coating [11]. The potassium was imported into the slags from the wood charcoal, along with Na, P, and S [11,23]. The phases from the olivine group are fayalite (proven in 3 samples) and kirschsteinite (proven in 1 sample). According to the results of the Mössbauer spectroscopy, uneven occupation of Fe^{2+} in 6-coordinated M1 and M2 positions was found in fayalite. The predominant occupancy of M1 with Fe^{2+} over M2 indicates that other divalent ions are involved in the M2 position. Position M2 is slightly bigger and much more distorted than M1, because of which the large sized Ca^{2+} ions are strongly connected to this position [24,25]. Since no other calcium-bearing phases were identified, it can be assumed that the calcium is completely incorporated into a Ca-bearing fayalite. The similar measured values of CaO (Table 1) for samples No. 116-1, 131-1, and 131-2 also correspond to the practically identical occupancy of the M2 position with Fe^{2+} (Table 3). The calcium isomorphism in fayalite is also confirmed by the shift of the X-ray [130] reflection—from 1.80Å to 1.84Å [26] (Figure 2). Mn^{2+} and Mg^{2+} can also be included in the M2 position [25]. The concentrations of MnO in the slag and ore are very similar, which indicates that Mn was introduced into the slag from the ore. The higher content of CaO (~3%) in sample No. 116-1 (Table 1) determines the crystallization of kirschsteinite instead of fayalite. A manganese phase—pyrolusite—was also proven in this sample. Pyrolusite is formed on contact with the ceramic coating of the furnace at a temperature above 900 °C in solid and/or partially liquid state [7,23]. The differences in the Fe^{2+} content in the M1 position (Table 3) show isomorphism in this position as well—Mg^{2+} is probably distributed in both M-positions [24,25].

The presence of olivine in the slags proves that there was enough quartz in the furnace to lead to its crystallization [5]. The similar concentrations of SiO_2 in all the examined samples suggest that no additional quartz was added in the furnace, as the ore contained

enough, which defines it as a self-fluxing ore. The reported changes in the amount of SiO_2 in the hematite ore and in the slags are due to the changes in the amount of quartz in the polymineral hematite ore in the individual parts of the deposit.

4.3. Produced Iron

The Fe_2O_3 content is lower in all of the slags but similar to the Fe_2O_3 content in the hematite ore. The differences in the Fe content in the slags compared to the ore was calculated: 7.98% for No. 116-1, 5.98% for No. 116-2, 3.39% for No. 131-1, and 8.65% for No. 131-2 (Tables 1 and 4), which correspond to the percentage of iron extracted from the ore.

Table 4. Produced iron % (calculated), Fe^{2+} (%) in oxide phases (measured), and viscosity index (calculated).

Sample	Produced Fe, Equivalent Mass %	Fe^{2+} in W, %	Fe^{3+} in Ma + G + Le, %	Viscosity Index
No. 116-1	7.98	33	15	0.28
No. 116-2	5.98	48	20	0.53
No. 131-1	3.39	40	21	0.32
No. 131-2	8.65	32	18	0.32

4.4. Factors Determining Produced Iron

The degree of iron recovery from the ore is determined by the temperature and redox conditions in the furnace, and by the viscosity of the liquid slag. The temperature and the redox conditions in the furnace depend on the construction of the furnace and the ratio of wood charcoal/ore, and can be determined by the phase composition of the slags. The viscosity of the liquid slag depends primarily on its chemical composition and temperature and can be calculated from the XRF results.

The wüstite phase suggests a reduction temperature of iron in the range 560–1200 °C, and fayalite between 1000 and 1100 °C [4]. Kirschsteinite crystallizes at a temperature below 900 °C [11]. Quartz reduces the reduction temperature of iron so that it occurs in the range 890–1140 °C [5,8]. Quartz is stable until reaching a temperature of around 890 °C, after which it transforms into tridymite. No reflections of tridymite were found in the PXRD patterns (Figure 3) but it is known that quartz peaks can be registered until around 1100 °C. In regard to this, it is possible for tridymite to be present in the slags, but in quantities below PXRD's detection range [7]. Leucite crystallizes at temperatures between 900 °C and 950 °C [27]. According to the temperature resistance of the described phases, it can be assumed that the lower limit of the temperature in the iron reduction furnace was about 900 °C, marked by the resistance of quartz and the crystallization temperature of leucite, and the upper limit was 1100 °C (marked by the maximum temperature at which quartz peaks are recorded and the crystallization temperature of fayalite). The temperature determined as an upper limit is also confirmed by the results obtained by Portilo et al. [4], according to whom, in slags in which there is an association of the olivine and wüstite phases, the temperature in the furnace was at a maximum of 1100° C.

It has been determined that the percentage of iron recovery by reduction is in the range between 10 and 20%, while the rest of the iron remains in the slag [4]. A significantly lower percentage of recovered iron was calculated for the investigated slags (Table 4). In relation to this, the presence of wüstite was proven in all the examined slags—a phase that crystallizes only in case of an excess of iron [5]. A large percentage of Fe^{2+} remaining in the slags was incorporated into wüstite (Table 3). These results indicate poorly controlled reduction conditions in the furnace and a correspondingly low degree of iron recovery from the ore [4]. The measured different contents of Fe^{2+} incorporated in wüstite indicate different degrees of decreased reduction control in the furnace. In order to determine the amount of iron initially included in the form of wüstite, it is necessary to take into account the amount of iron included in maghemite, magnetite, goethite, and lepidocrocite, since:

(i) maghemite and magnetite are transformation products of $Fe_{1-x}O$ (wüstite) to γ-Fe_2O_3 (maghemite) and/or subsequent formation of $Fe_{3-x}O_4$ (magnetite) under appropriate redox conditions during the solidification of the slag [12]; and (ii) goethite and lepidocrocite, which are typical minerals from the weathering process of wüstite [7,12] (Table 4). There is a decrease in the measured amount of iron incorporated in these phases and a parallel increase in the calculated amount of iron extracted from the ore. An exception is sample No. 116-2, in which the content of iron incorporated into wüstite is the highest, but also the percentage of extracted iron is high compared to sample No. 131-1, in which the values of SiO_2 and Fe_2O_3 are similar (Table 1). This reverse relationship is probably related to the higher CaO content in sample No. 116-2. CaO is known to increase the basicity and decrease the viscosity of the liquid slag [28] and the low viscosity aids the separation of iron from the slag, i.e., the percentage of extracted iron increases [29]. Various methods have been proposed for calculating the viscosity of modern blast furnace slags obtained in the iron production process. Viscosity calculations are based on calculating the viscosity index using the ratio of basic to acidic oxides. The higher this viscosity index is, the less viscous the liquid slags are [28,29]. The viscosity index can be calculated using the formula sum of basic oxides to sum of acidic oxides (mass %): ($CaO + Fe_2O_3 + MgO + MnO + K_2O + Na_2O + TiO_2$)/($SiO_2 + Al_2O_3$). The viscosity index of modern iron slags calculated by this formula is usually in the range 0.5–1 [29]. The formula proposed by Bachmann [29] was formulated for modern metallurgical blast furnace slags in which the iron content does not exceed one percent [28] and is part of the liquid slag. In the direct iron reduction method, the slag is the only liquid component in the system and the iron is in solid state [5,9], which requires the iron content to be excluded from the formula. For the examined slags, the viscosity index was calculated according to the formula ($CaO + MgO + MnO + K_2O + Na_2O + TiO_2$)/($SiO_2 + Al_2O_3$) and the results are presented in Table 4. The viscosity index values for samples No. 116-1, No. 131-1, and No. 131-2 are lower than 0.5 (below the values for modern slags), and the value for sample No. 116-2 falls within the viscosity limits of modern metallurgical slags (Table 4). In modern iron metallurgy, calcium-containing flux is normally added, most often in the form of fluorite (CaF_2), calcite $CaCO_3$, or dolomite ($CaMg(CO_3)_2$), which lowers the viscosity of the slags [28]. Therefore, it can be assumed that the higher viscosity of No. 116-1, No. 131-1, and No. 131-2 is related to the lower content of CaO, and that, conversely, the higher content of CaO in No. 116-2 lowers the viscosity of the liquid slag. An increase in the viscosity of the liquid slag reduces the aggregation of solid iron, which also leads to a decrease in the percentage of extracted iron in the reduction process [29]. However, the degree of iron recovery depends also on the temperature and the redox conditions in the furnace. In this regard, no clear relationship between the viscosity index and the extracted iron was found for the four samples (Table 4). The same furnace operating temperature range was determined for all samples, but with a different degree of control over the reduction conditions, evidenced by the different content of Fe^{2+} incorporated into the wüstite. This allows for the establishment of a relationship between the extractability of iron from the ore, the content of Fe^{2+} included in wüstite, and the viscosity index. Equal viscosity index values were calculated for samples No. 131-1 and No.131-2, and it was found that an increase in Fe^{2+} included in wüstite of 8% lead to a decrease in the percentage of extracted iron of 39% (Table 4). In sample No. 116-2, Fe^{2+} included in wüstite is also 8% more than that in sample No. 131-1, but the percentage of extracted iron is also higher by 43%, i.e., the increase in the liquid slag's viscosity index by 0.21 significantly increases the degree of iron recovery, even with worse reduction conditions in the furnace.

5. Conclusions

All investigated slags are furnace bottom slags, a waste product of metallurgical activity in a bloomery furnace. No tapped slags were found in both archaeological sites, which suggests the use of furnaces with imperfect designs—without openings for draining the ore.

Iron reduction was performed in a temperature range of 900-1100 °C, which was possible without the addition of flux, since the ore used for the metallurgical process in both sites was defined as self-fluxing hematite ore. Furnace conditions were not sufficiently reducing and constant due to uncontrolled air supply and/or low charcoal/ore ratio in the furnace. It is possible that the inconsistent and poor ventilation control is also related to the simpler design of the furnaces—with only one opening for air supply. On the other hand, the landscape of the settlements does not allow the use of wind-powered furnaces.

The low temperature in the furnace, the different and poorly controlled reduction conditions, as well as the low viscosity index determine a low percentage of extracted iron from the ore (from 3.39 to 8.65%). The established relationship between percentage of iron extraction from ore, content of Fe^{2+} incorporated in wüstite, and viscosity index shows that, in a bloomery furnace: (i) when the temperature and viscosity conditions are equal for the liquid slag, the reduction environment has a decisive influence on the percentage of extracted iron—the weaker reduction environment (defined as 8% increased iron content included in wüstite) leads to a 39% decrease in the percentage of extracted iron; (ii) when the temperature and redox conditions are equal, the viscosity index has a controlling role for the percentage of extracted iron (an increase in the viscosity index by 0.21 increases the extracted iron by 43%).

The archaeological sites from which the studied slags were collected were dated via ceramics to the Late Iron and Roman Ages (Sladak Kladenets site) and Late Antiquity and Middle Ages (Malko Dryanovo site). The obtained results suggest that the metallurgical process conducted in both sites was implemented according to technology from the earliest archaeological period. In this regard, it can be assumed with high probability that if the metallurgical process continued in the later periods, the original iron mining technology was preserved and passed on to the later archaeological eras. A further contribution to the reconstruction of the economic situation is the conclusion that the two unfortified settlements were iron producers and workshops for the production of common tools and their distribution on a local scale. This confirms, but also builds on, the general idea of the great possibilities of non-urban Roman settlements of 3rd-4th c AD for autarchy, but also for regional exchange.

Author Contributions: Conceptualization, B.K. and B.D.; Sample preparation, B.K.; XRF and PXRD analysis, B.K. and K.M.; Mössbauer spectroscopy, D.P. and Z.C.-Z. writing—original draft preparation, B.K., D.P. and Z.C.-Z.; writing—review and editing, K.M. and B.D.; funding acquisition, B.K. All authors have read and agreed to the published version of the manuscript.

Funding: This research was funded by Bulgarian National Science Fund, grant number KP-06-N39/9 (B.K., B.D).

Data Availability Statement: The data presented in this study are available on request from the corresponding author.

Acknowledgments: The authors gratefully acknowledge New Bulgarian University, the Department of Natural Sciences and the Geology laboratory—BF.

Conflicts of Interest: The authors declared no conflict of interest.

References

1. Bayley, J.; Dungworth, D.; Paynter, S.C. *Archaeometallurgy: Guidelines for Best Practice*; Historic England: England, UK, 2015.
2. Williams, A. *The Knight and the Blast Furnace: A Histoty of the Metallurgy of Armour in the Middle Ages and the Early Modern Period*; Brill: Leiden, The Netherlands, 2003.
3. Larreina-Garcia, D.; Li, Y.; Liu, Y.; Martinón-Torres, M. Bloomery iron smelting in the Daye County (Hubei): Technological traditions in Qing China. *Archaeol. Res. Asia* **2018**, *16*, 148–165. [CrossRef]
4. Portillo, H.; Zuluaga, M.C.; Ortega, L.A.; Alonso-Olazabal, A.; Murelaga, X.; Martinez-Salcedo, A. XRD, SEM/EDX and micro-Raman spectroscopy for mineralogical and chemical characterization of iron slags from the Roman archaeological site of Forua (Biscay, North Spain). *Microchem. J.* **2018**, *138*, 246–254. [CrossRef]

5. Portillo-Blanco, H.; Zuluaga, M.C.; Ortega, L.A.; Alonso-Olazabal, A.; Cepeda-Ocampo, J.J.; Martínez Salcedo, A. Mineralogical characterization of slags from the Oiola site (Biscay, Spain) to assess the development in bloomery iron smelting technology from the Roman period to the Middle Ages. *Minerals* **2020**, *10*, 321. [CrossRef]
6. Roberts, B.W.; Thornton, C.P. *Archaeometallurgy in Global Perspective: Methods and Syntheses*; Springer: New York, NY, USA, 2014. [CrossRef]
7. Bitay, E.; Kacsó, I.; Tănăselia, C.; Toloman, D.; Borodi, G.; Pánczél, S.-P.; Kisfaludi-Bak, Z.; Veress, E. Spectroscopic characterization of iron slags from the archaeological sites of Brâncoveneşti, Călugăreni and Vătava located on the Mureş County (Romania) Sector of the Roman Limes. *Appl. Sci.* **2020**, *10*, 5373. [CrossRef]
8. Manasse, A.; Mellini, M. Chemical and textural characterisation of medieval slags from the Massa Marittima smelting sites (Tuscany, Italy). *J. Cult. Herit* **2002**, *3*, 187–198. [CrossRef]
9. Tylecote, R.F. *A History of Metallurgy*, 2nd ed.; Maney: For the institute of material: London, UK, 2002.
10. Friede, H.; Hejja, A.; Koursaris, A. Arhaeo-metallurgical studies of iron smelting slags from prehistoric sites in Southern Africa. *J. S. Afr. Inst. Min. Metall.* **1982**, *82*, 38–48.
11. Török, B.; Gallina, Z.; Kovács, Á.F. Kristály, Early medieval iron bloomery centre at Zamárdi (Hungary), Complex archaeometrical examinations of the slags. *Archeol. Rozhl.* **2018**, *70*, 404–420.
12. Di Bella, M.; Aleo Nero, C.; Chiovaro, M.; Italiano, F.; Leonetti, F.; Marcianò, G.; Quartieri, S.; Romano, D.; Sabatino, G. Archaeometric study of the Hellenistic metallurgy in Sicily: Mineralogical and chemical characterization of iron slags from Punic Panormos (Palermo, Italy). *Mediterr. Archaeol. Archaeom.* **2018**, *18*, 127–139. [CrossRef]
13. Chernih, E.N. *Mining and Metallurgy in Ancient BULGARIA*; BAS Publishing House: Sofia, Bulgaria, 1978.
14. Dumanov, B. *Archaeology of the Old Iron Mining on the Lower Danube and in the Stara Planina Mountain Region—Roman Imperial Epoch-End of the XVIII Century*; New Bulgarian University: Sofia, Bulgaria, 2021.
15. Tsankov, T.; Philipov, L.; Katskov, N. *Explanatory Note to a Geological Map of Bulgaria M 1:100,000, Kazanlak Map Sheet*; ET Avers: Sofia, Bulgaria, 1995.
16. Kanurkov, G. *Iron Ore Deposits in Bulgaria*; Tehnika: Sofia, Bulgaria, 1988.
17. Uzunov, Z.; Dimitrova, I.; Dumanov, B. Results from the field archeological excavations of archeological sites in the working area. In *SARCHUS-AIR. Localization and Experimental Reconstruction of Ancient Roads and Habitats*; Dumanov, B., Ed.; Askoni Izdat.: Sofia, Bulgaria, 2017; pp. 37–49.
18. *PDF (Powder Diffraction File)*; ICDD: Newtown Square, PA, USA, 2001.
19. Wyckoff, R.W.G. *Crystal Structures*; Interscience Publishers: New York, NY, USA, 1963.
20. Cornell, R.M.; Schwertmann, U. *The Iron Oxides: Structure, Properties, Reactions, Occurrences and Uses*, 2nd ed.; Wiley-VCH: Weinheim, Germany, 2003. [CrossRef]
21. Geiger, C.A.; Vielreicher, N.M.; Dachs, E. Are the thermodynamic properties of natural and synthetic Mg_2SiO_4-Fe_2SiO_4 olivines the same? *Am. Miner.* **2021**, *106*, 317–321. [CrossRef]
22. Eibschütz, M.; Ganiel, U. Mössbauer studies of Fe^{2+} in paramagnetic fayalite (Fe_2SiO_4). *Solid State Commun.* **1967**, *5*, 267–270. [CrossRef]
23. Kramar, S.; Lux, J.; Pristacz, H.; Mirtič, B.; Rogan-Šmuc, N. Mineralogical and geochemical characterization of Roman slag from the archaeological site near Mosnje (Slovenia). *Mater. Technol.* **2015**, *49*, 343–348. [CrossRef]
24. Davidson, P.M.; Mukhopadhyay, D.K. Ca-Fe-Mg olivines: Phase relations and a solution model. *Contrib. Miner. Pet.* **1984**, *86*, 256–263. [CrossRef]
25. Dyar, M.D.; Sklute, E.C.; Menzies, O.N.; Bland, P.A.; Lindsley, D.; Glotch, T.; Lane, M.D.; Schaefer, M.W.; Wopenka, B.; Klima, R.; et al. Spectroscopic characteristics of synthetic olivine: An integrated multi-wavelength and multi-technique approach. *Am. Mineral.* **2009**, *94*, 883–898. [CrossRef]
26. Wyderko, M.; Mazanek, E. The mineralogical characteristics of calcium-iron olivines. *Mineral. Mag. J. Mineral. Soc.* **1968**, *36*, 955–961. [CrossRef]
27. Tošić, M.B.; Mitrović, M.M.; Dimitrijević, R.Ž. Crystallization of leucite as the main phase in aluminosilicate glass with low fluorine content. *J. Mater. Sci.* **2000**, *35*, 3659–3667. [CrossRef]
28. Allibert, M. *Slag Atlas*, 2nd ed.; Verlag Stahleisen GmbH: Düsseldorf, Germany, 1995.
29. Bachmann, H.G. *The Identification of Slags from Archeological Sites*; Occasional Publication No. 6; Institute of Archeology: London, UK, 1982; pp. 1–37.